Synthesis of Urea-Based Inhibitors as Active Site Probes of Glutamate Carboxypeptidase II: Efficacy as Analgesic Agents

Alan P. Kozikowski,*,† Jiazhong Zhang,† Fajun Nan,† Pavel A. Petukhov,† Ewa Grajkowska,‡ Jarda T. Wroblewski,‡ Tatsuo Yamamoto,§ Tomasz Bzdega,# Barbara Wroblewska,# and Joseph H. Neale#

Drug Discovery Program, Department of Medicinal Chemistry and Pharmacognosy, 539 College of Pharmacy, University of Illinois at Chicago, 833 South Wood Street, Chicago, Illinois 60612, Department of Pharmacology, Georgetown University Medical Center, 3970 Reservoir Road, N.W., Washington, D.C. 20057, Departments of Anesthesiology and Neurobiology, Graduate School of Medicine, Chiba University, Chiba 260-8670, Japan, and Department of Biology, Georgetown University, Washington, D.C. 20057

Received December 23, 2003

The neuropeptidase glutamate carboxypeptidase II (GCPII) hydrolyzes *N*-acetyl-L-aspartyl-L-glutamate (NAAG) to liberate *N*-acetylaspartate and glutamate. GCPII was originally cloned as PSMA, an M_r 100 000 type II transmembrane glycoprotein highly expressed in prostate tissues. PSMA/GCPII is located on the short arm of chromosome 11 and functions as both a folate hydrolase and a neuropeptidase. Inhibition of brain GCPII may have therapeutic potential in the treatment of certain disease states arising from pathologically overactivated glutamate receptors. Recently, we reported that certain urea-based structures act as potent inhibitors of GCPII (*J. Med. Chem.* **2001**, *44*, 298). However, many of the potent GCPII inhibitors prepared to date are highly polar compounds and therefore do not readily penetrate the blood−brain barrier. Herein, we elaborate on the synthesis of a series of potent, urea-based GCPII inhibitors from the lead compound **3** and provide assay data for these ligands against human GCPII. Moreover, we provide data revealing the ability of one of these compounds, namely, **8d**, to reduce the perception of inflammatory pain. Within the present series, the γ-tetrazole bearing glutamate isostere **7d** is the most potent inhibitor with a K_i of 0.9 nM. The biological evaluation of these compounds revealed that the active site of GCPII likely comprises two regions, namely, the pharmacophore subpocket and the nonpharmacophore subpocket. The pharmacophore subpocket is very sensitive to structural changes, and thus, it appears important to keep one of the glutamic acid moieties intact to maintain the potency of the GCPII inhibitors. The site encompassing the nonpharmacophore subpocket that binds to glutamate's α-carboxyl group is sensitive to structural change, as shown by compounds **6b** and **7b**. However, the other region of the nonpharmacophore subpocket can accommodate both hydrophobic and hydrophilic groups. Thus, an aromatic ring can be introduced to the inhibitor, as in **8b** and **8d**, thereby increasing its hydrophobicity and thus potentially its ability to cross the blood−brain barrier. Intrathecally administered **8d** significantly reduced pain perception in the formalin model of rat sensory nerve injury. A maximal dose of morphine (10 mg) applied in the same experimental paradigm provided no significant increase in analgesia in comparison to **8d** during phase 1 of this pain study and modestly greater analgesia than **8d** in phase 2. These urea-based inhibitors of GCPII thus offer a novel approach to pain management.

Introduction

L-Glutamate is one of the most abundant excitatory neurotransmitters found in the mammalian brain. Through its actions on ionotropic and metabotropic receptors, glutamate plays an important role in a variety of physiological functions including learning, memory, and developmental plasticity. Excessive glutamatergic transmission has been implicated in the pathogenesis of a host of neurological disorders, including excitotoxic cell death associated with ischemia and central nervous system trauma, inflammatory and neuropathic pain, and chronic neurodegenerative diseases. Over the past decade, considerable effort has been given to the discovery of selective agonists and antagonists of glutamate receptors that possess therapeutic potential for these conditions. Although several drugs designed to attenuate the pathological consequences of excessive glutamate activation have been shown to reduce injury in experimental models of cerebral ischemia, so far none of these compounds has proven to be effective in the clinical treatment of stroke.[1]

N-Acetyl-L-aspartyl-L-glutamate (NAAG), a major peptide neurotransmitter in the mammalian nervous system,[2] acts as an agonist at group II metabotropic glutamate receptors on neurons and glia.[3] The neuropeptidase glutamate carboxypeptidase II (GCPII) is an extracellular enzyme that hydrolyzes NAAG to *N*-acetylaspartate and glutamate following the release of the peptide into the synaptic space.[4] There appears to be a high level of NAAG metabolism in the brain, and inhibition of the peptidase activity has been shown to

* To whom correspondence should be addressed. Phone: 202 687 0686. Fax: 202 687 5065. E-mail: kozikowa@uic.edu.
† University of Illinois at Chicago.
‡ Georgetown University Medical Center.
§ Chiba University.
# Georgetown University.

10.1021/jm0306226 CCC: $27.50
Published on Web 03/02/2004

substantially reduce extracellular levels of glutamate under conditions of intense synaptic release.[5] Thus, the inhibition of peptidase activity against NAAG has the potential to provide protection in clinical conditions in which glutamate mediates and mGluR3 activation reduces clinical pathology.[5a,6] Reduced blood flow to the brain as occurs during stroke and cardiac arrest results in a high level of excitatory transmitter release in the brain, including the release of glutamate and NAAG. The high glutamate levels are responsible for a cascade of events that lead to a delayed nerve cell death. Additionally, glutamate has long been recognized as a spinal sensory transmitter with a significant role in pain perception and the physiological events that mediate chronic pain perception associated with inflammation or peripheral nerve irritation (allodynia). Activation of group II mGluRs (mGluR2 and mGluR3) has been shown to reduce perception of this type of pain.[7] For these reasons, decreasing extracellular glutamate and increasing the concentration of the group II agonist NAAG by inhibition of brain peptidase activity against this peptide represent a significant new therapeutic strategy.

2-PMPA (**1**) is a potent inhibitor of GCPII[8] and has been shown to provide significant protection against injury in rats after transient middle cerebral artery occlusion.[5a] In this model system, 2-PMPA substantially reduced the large increase in extracellular glutamate levels that occurs immediately after induction of ischemia while having no detectable effect on glutamate levels under normal conditions. 2-PMPA also has been found to reduce the perception of chronic pain in rodent models.[9] As a therapeutic target, GCPII inhibition has been suggested to have potential benefits over the existing receptor-based strategies because it represents an upstream mechanism for regulation of synaptic glutamate that could reduce transmission at a number of glutamatergic receptors rather than inhibiting a single receptor subtype. Equally important, NAAG is colocalized in neurons with small amine transmitters, including glutamate, GABA, acetylcholine, and dopamine,[10] and it has been shown to act on presynaptic mGluR3 receptors to inhibit transmitter release.[11] Thus, endogenous NAAG may play a significant role in inhibiting the release of glutamate in pathological conditions where excess glutamate is a central factor.

Our studies are directed toward the development of GCPII inhibitors using NAAG as the lead compound.[12] We designed and synthesized a dually acting ligand, 4,4′-phosphinicobis(butane-1,3-dicarboxylic acid) (**2**), which acts both as an mGluR3 selective agonist (~30 μM) and as a potent inhibitor of GCPII (21.7 ± 2.1 nM). Starting from this lead compound, we then designed and synthesized several urea-based ligands, including **3** and **4**, which display potent inhibitory activity toward GCPII and possess a strong neuroprotective action. However, many of the potent GCPII inhibitors (shown in Figure 1) prepared to date are highly polar compounds and as such may not readily penetrate the blood−brain barrier. Because of the relative ease with which compounds of this structural type can be prepared, we chose to synthesize additional examples to elucidate their SAR, which may, in turn, lead to the discovery of more potent

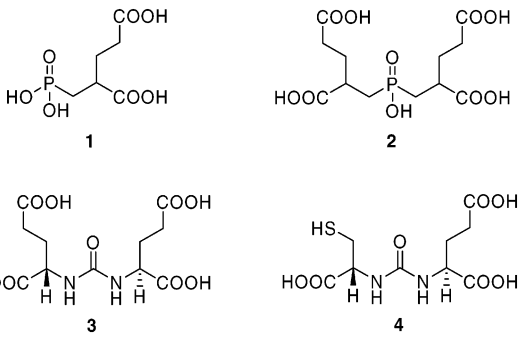

Figure 1. Previously reported GCPII inhibitors.

GCPII inhibitors with enhanced lipophilicity. The synthesis, enzyme inhibitory activities, and analgesic qualities of our new compounds are described herein.

Additionally, in light of the identity of human GCPII with prostate specific membrane antigen, a type II transmembrane glycoprotein highly expressed in prostate hyperplasia, inhibitors with high affinity for the active site of GCPII may also find applications in prostate tumor diagnosis and therapy.

Chemistry

The compounds that have been prepared are shown in Figure 2. In our previous work,[12b] we have demonstrated the specificity of GCPII for ligands containing *S*-configured amino acids (or *R* in the case of cysteine) by comparing the activity of compound **3** with that of its two stereoisomers. We therefore limited our present efforts to the synthesis of analogues possessing the *S*-configuration in both amino acid moieties. In general, symmetrical ureas were obtained by treating the appropriate amino acid benzyl esters (in free form or as their tosylates), which were prepared according to a published procedure,[13] with triphosgene/Et_3N. The unsymmetrical ureas were prepared through the reaction of isocyanate **11**, generated in situ from the tosylate salt of glutamic acid dibenzyl ester and triphosgene/Et_3N, with the second amino acid benzyl ester. The benzyl ester intermediates were then converted to the free acids by catalytic hydrogenation (Scheme 1).

To construct the bioisosteric tetrazole analogues, the 2-cyanoethyl group was initially chosen as the N^1-protecting group of the tetrazole. Starting from commercially available α-benzyl-*N*-Boc-L-glutamate **12**, the tetrazole moiety was elaborated according to a published procedure as shown in Scheme 2.[14] Deprotection of **14** with CF_3COOH afforded the free amine, which was used to prepare symmetrical and unsymmetrical tetrazole-containing urea intermediates following the procedures described above (Schemes 2 and 3). Hydrogenolysis of the resulting benzyl ester intermediates afforded the cyanoethyl-protected tetrazole acids **6c** and **7c**, which were then further deprotected with DBU to afford, after purification on a cation exchange column (Dowex-50WX8-400), the free tetrazole acids **6d** and **7d**. Analogues **6a**,**b** and **7a**,**b**, in which one or both α-carboxyl groups are replaced by tetrazole moieties, were prepared in a similar fashion using γ-benzyl-*N*-Boc-L-glutamate as the starting material. To avoid the cation exchange treatment necessary after cleavage of the cyanoethyl group, we switched to benzyl as the N^1-protecting group of the tetrazole. The final deprotection could then be

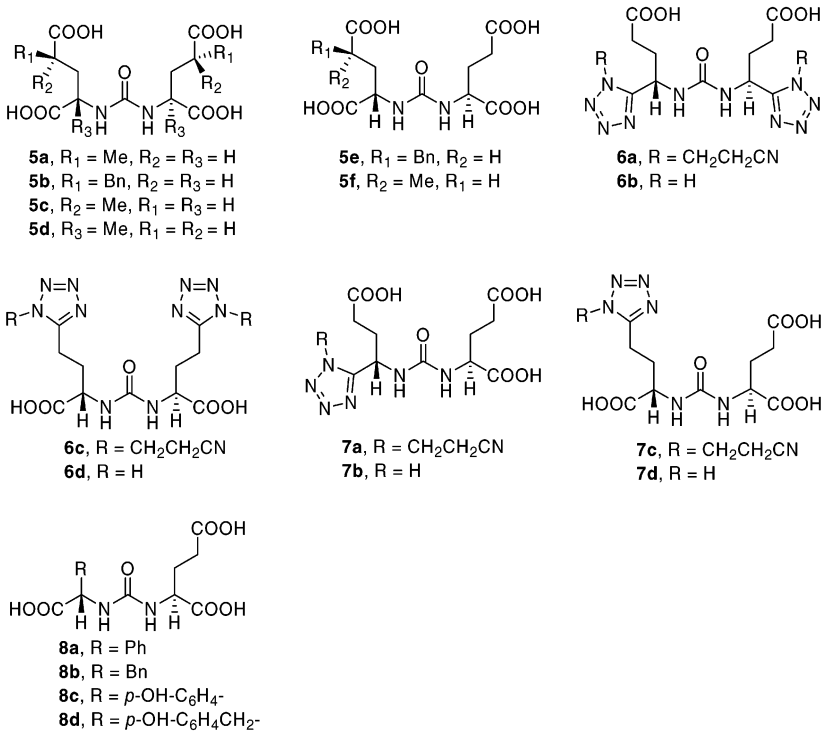

Figure 2. New inhibitors synthesized in the present study.

Scheme 1. Synthetic Route to Compounds **5e**,**f**[a]

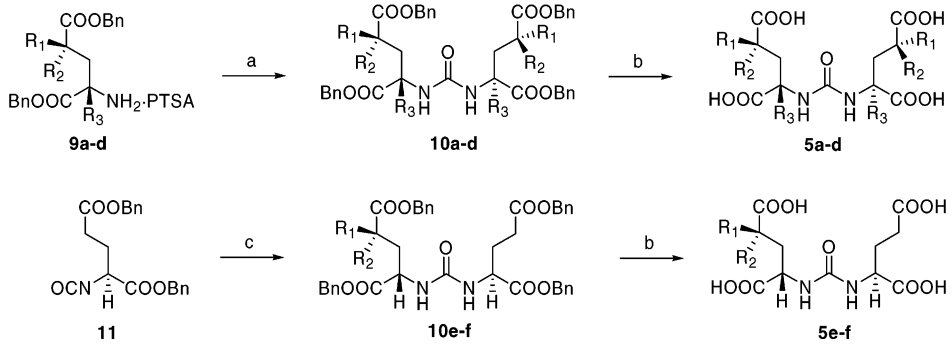

[a] Reagents: (a) triphosgene, Et_3N, CH_2Cl_2, −78 °C to room temperature; (b) H_2, 20% $Pd(OH)_2$/C, *t*-BuOH; (c) **5b** or **5c**, Et_3N, CH_2Cl_2.

Scheme 2. Synthetic Scheme for the Preparation of **6d**[a]

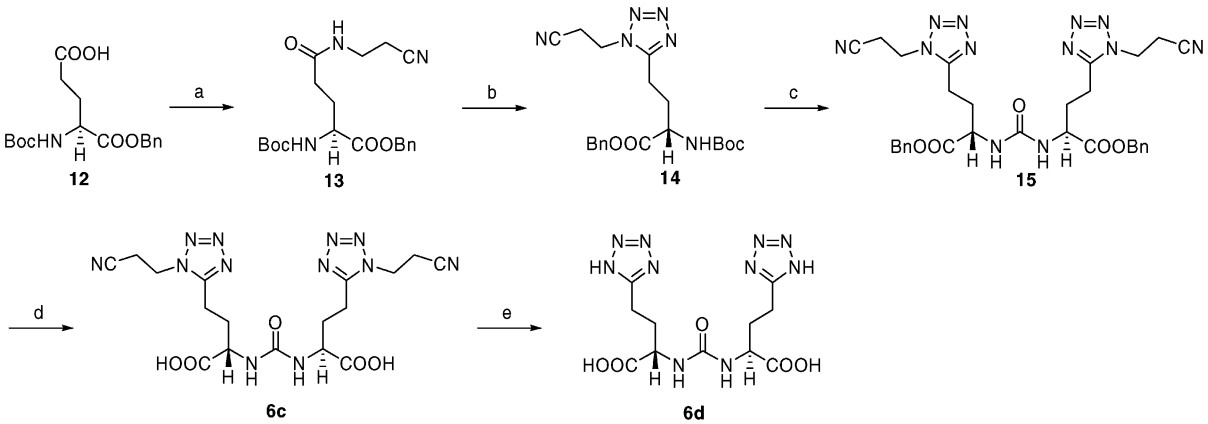

[a] Reagents: (a) 3-aminopropionitrile fumarate, BOP, Et_3N, DMF; (b) $TMSN_3$, DIAD, Ph_3P, CH_3CN; (c) (i) CF_3COOH, CH_2Cl_2; (ii) triphosgene, Et_3N, CH_2Cl_2, −78 °C to room temperature; (d) H_2, 20% $Pd(OH)_2$/C, *t*-BuOH; (e) DBU, CH_2Cl_2, 2 h.

carried out in a single step by catalytic hydrogenation (Scheme 4).

Finally, a series of urea analogues containing aromatic substituents were prepared as shown in Scheme 5 using commercially available amino acids. The benzyl esters of the aromatic amino acids were reacted with isocyanate **11** to give urea intermediates **21a**−**d**. Catalytic hydrogenation of the resulting intermediates pro-

Scheme 3. Synthetic Scheme for the Preparation of **7d**[a]

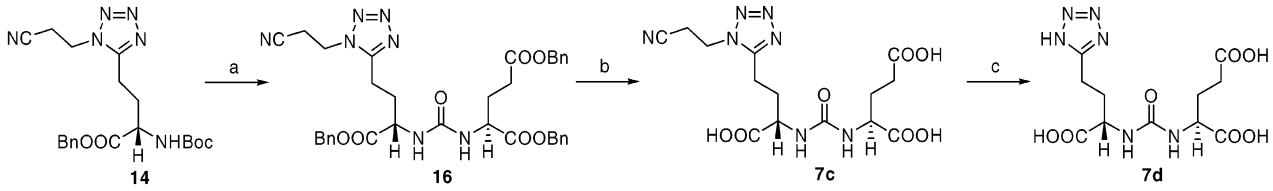

[a] Reagents: (a) (i) CF_3COOH, CH_2Cl_2; (ii) isocyanate **11**, Et_3N, CH_2Cl_2; (b) H_2, 20% $Pd(OH)_2/C$, *t*-BuOH, 1 h; (c) DBU, CH_2Cl_2, 2 h.

Scheme 4. Alternative Synthetic Scheme for the Preparation of **6d**[a]

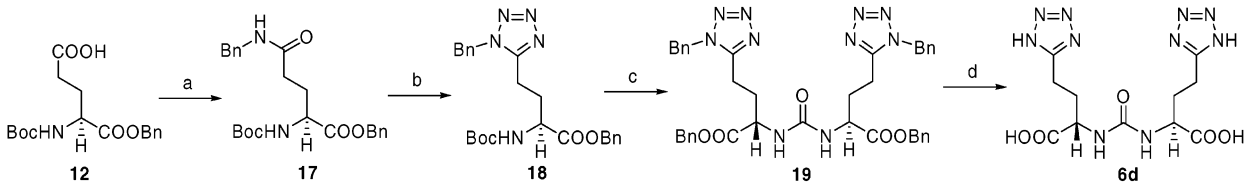

[a] Reagents: (a) $BnNH_2$, BOP, Et_3N, DMF; (b) $TMSN_3$, DIAD, Ph_3P, CH_3CN; (c) (i) CF_3COOH, CH_2Cl_2, room temp, 1 h; (ii) triphosgene, Et_3N, CH_2Cl_2, −78 °C to room temperature; (d) H_2, 20% $Pd(OH)_2/C$, *t*-BuOH.

Scheme 5. Route to **8a**−**d**[a]

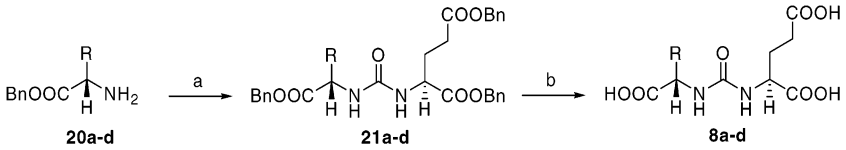

[a] Reagents: (a) isocyanate **11**, Et_3N, CH_2Cl_2, overnight; (b) H_2, 20% $Pd(OH)_2/C$, *t*-BuOH.

vided the free acids **8a**−**d**. It should be noted here that for compound **8a**, partial epimerization occurred when L-phenylglycine benzyl ester was used to prepare the urea as evidenced by the ^{13}C NMR spectra of the tribenzyl ester intermediate and the final free acid. However, epimerization can be avoided by reacting the isocyanate **11** directly with free L-phenylglycine.

Results and Discussion

All new compounds were tested for their ability to inhibit human GCPII using conditions described in the Experiment Section. For comparison purposes, 2-PMPA **1** and urea **3** were assayed in parallel with the compounds reported herein and found to have K_i values of 1.4 and 8.0 nM, respectively. The inhibitory activities of the new compounds and their calculated log *P* values are listed in Table 1 with full dose−response curves shown in Figure 4. All four symmetrical alkylated urea analogues **5a**−**d** were found to be almost inactive, with K_i values of greater than 300 nM against expressed human GCPII. In comparison, the unsymmetrical monoalkylated ureas **5e** and **5f** showed some inhibitory activity with K_i values of 95.3 and 14.4 nM, respectively. Thus, incorporation of alkyl substituents into the urea structure decreases enzyme inhibitory activity.

One possible explanation is that the alkyl substituent cannot be sterically accommodated by the binding pocket or alter the inhibitor's conformation and consequently the location of the carboxylic acid group. Our modeling study[15] of the active site of GCPII complexed with the phosphonate/phosphinate inhibitors **1** and **2** indicates that there are two binding regions in the enzyme active site, one for each pentanedioic acid moiety. The two carboxyl groups of one of these moieties interact with the residues of the enzyme through hydrogen bonds in one region, namely, the pharmocophore subpocket. Within the other region, referred to as the nonpharmocophore subpocket, another pentanedioic acid moiety can interact with the enzyme active site through hydrogen bonding or hydrophobic interactions. Each region has two binding sites as shown in Figure 3. On the basis of the inhibitory data obtained in the present work, we can hypothesize that the pharmacophore subpocket has low tolerance to structural changes of the inhibitors while the nonpharmacophore subpocket has a higher tolerance to structural changes. For good enzyme inhibitory action, both of the subpockets should be engaged by the inhibitor. Therefore, it appears necessary to keep one glutamic acid unit intact.

Table 1. Inhibitory Activity of Urea Analogues against Expressed Human GCPII

compd	ClogP [a]	K_i (nM)	SEM
1	−1.38	1.4	±0.09
3	−1.54	8.0	±0.6
5a	−0.70	1285	±67
5b	+ 2.71	392	±56
5c	−0.70	1109	±62
5d	−0.63	939	±37
5e	+ 0.59	95.3	±7.7
5f	−1.12	14.4	±0.7
6a	−4.50	>100000	
6b	−4.62	4388	±211
6c	−3.66	4434	±165
6d	−3.78	14.9	±0.8
7a	−3.02	2711	±211
7b	−3.08	335	±35
7c	−2.60	5.3	±0.3
7d	−2.66	0.9	±0.05
8a	−0.07	2.1	±0.1
8b	+ 0.43	12.0	±0.9
8c	−0.55	5.9	±0.3
8d	−0.05	3.0	±0.2

[a] Calculated using the KowWin program (http://esc.syrres.com/interkow/kowdemo.htm).

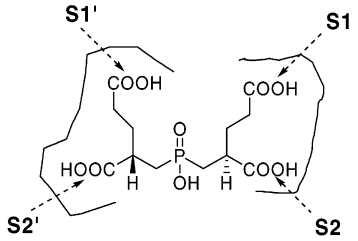

Figure 3. Proposed binding domains of GCPII inhibitors in the active site of GCPII.

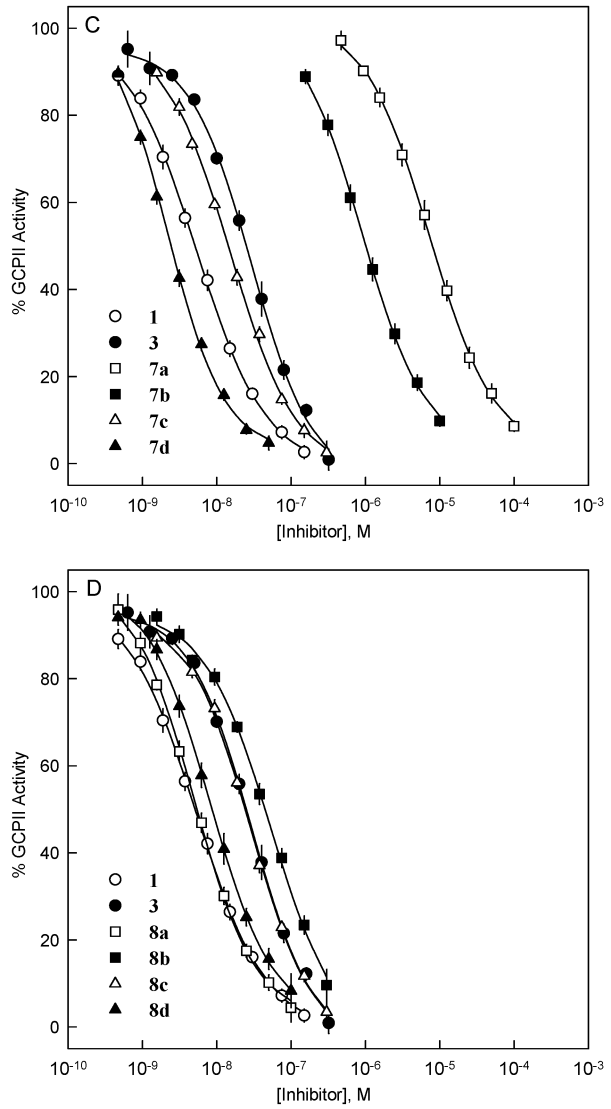

Figure 4. Inhibition of human GPCII by urea analogues. Dose−response curves of the indicated compounds were generated in the presence of 3 μM NAAG, as described in the methods section. In each figure, 2-PMPA (**1**) and lead compound **3** were used as the reference compounds. Points represent the mean ± SEM from 8 to 12 experiments.

Because the introduction of even a small alkyl substituent (analogue **5f**) reduced activity, we turned our attention to the preparation of bioisosteres of the lead urea **3**. The tetrazole moiety is an often-used surrogate for the carboxyl group. First, we examined the activity of the symmetrical N-protected and unprotected tetrazole-containing urea analogues **6a**−**d**. Among those compounds, only compound **6d** exhibited relatively high binding affinity to the enzyme, with a K_i value of 14.9 nM, while the other three were found to be almost inactive. The low activity of the 2-cyanoethyl protected tetrazoles **6a** and **6c** is readily explained by steric interference in the low-tolerance pharmacophore subpocket. The result that the α-tetrazole **6b** was almost inactive while the γ-tetrazole **6d** was fairly active may indicate that one part (S1 or S1′) of the enzyme active site can accommodate a limited amount of steric bulk while the other part (S2 or S2′) is intolerant even of minor steric effects. To obtain further insight into the active site of the enzyme, the unsymmetrical tetrazole-containing ureas **7a**−**d** were prepared. Compound **7d** exhibits high inhibitory activity with a K_i value of 0.9 nM. Interestingly, the 2-cyanoethyl-protected γ-tetrazole **7c** is also fairly potent (K_i = 5.3 nM). This result supports our hypothesis that the nonpharmacophore subpocket (site S1′) is relatively large. The free and 2-cyanoethyl-protected α-tetrazoles **7a** and **7b** exhibit low activity, suggesting that the sites S2 and S2′ are intolerant to structural changes.

The above results indicate that only the sites S1 and S1′ in the enzyme active site permit structural modifications that increase steric bulk. In particular, the site S1′ in the nonpharmacophore subpocket is tolerant of relatively large hydrophobic groups, as demonstrated by the relatively high activity of compound **7c**, whereas only small changes are tolerated at the site S1 in the pharmacophore subpocket. In response to this finding, we investigated the introduction of an aromatic ring into one of the amino acid moieties, which would increase the lipophilicity of the inhibitors and possibly facilitate their penetration of the blood−brain barrier. The unsymmetrical phenyl-substituted ureas **8a** and **8b** were prepared from commercially available amino acids. To our pleasant surprise, both compounds are fairly potent inhibitors of expressed GCPII, with K_i values of 2.1 and 12.0 nM, respectively. Compound **8b** is particularly interesting in light of its positive ClogP value (+0.43). Since the S1′ subpocket readily accommodates certain hydrophilic groups, as demonstrated by compounds **2, 3**, **6d**, and **7d**, we next prepared the *p*-hydroxylated ureas **8c** and **8d** from the corresponding amino acids. Both exhibit high GCPII inhibitory activity, with K_i values of 5.9 and 3.0 nM, respectively.

Because a decision was made to explore the effects of ligand **8d** in an animal model of pain, we chose to better assess the druglikeness of **8d**. Both its Caco2 and blood−brain barrier (BBB) permeability were calculated and compared to those of certain known drugs. The results of these calculations employing commercial software available from Tripos are shown in Figure 5. According to the calculations, compound **8d** has Caco2 and BBB permeability comparable to that of cefotaxime, chlortetracycline, and dimethylchlortetracycline. At least one of these drugs, cefotaxime, a well-known antibiotic for the treatment of meningitis, penetrates the BBB.

In Vivo Assay. Formalin Test. In the saline-treated rats, a subcutaneous injection of formalin in the footpad resulted in a highly reliable biphasic display of flinching of the injected paw (Figure 6), and this behavior was comparable to that previously reported.[9a] Intrathecal administration of **8d** 10 min prior to formalin injection decreased both the phase 1 and phase 2 flinching response in a dose-dependent manner (phase 1, $p <$

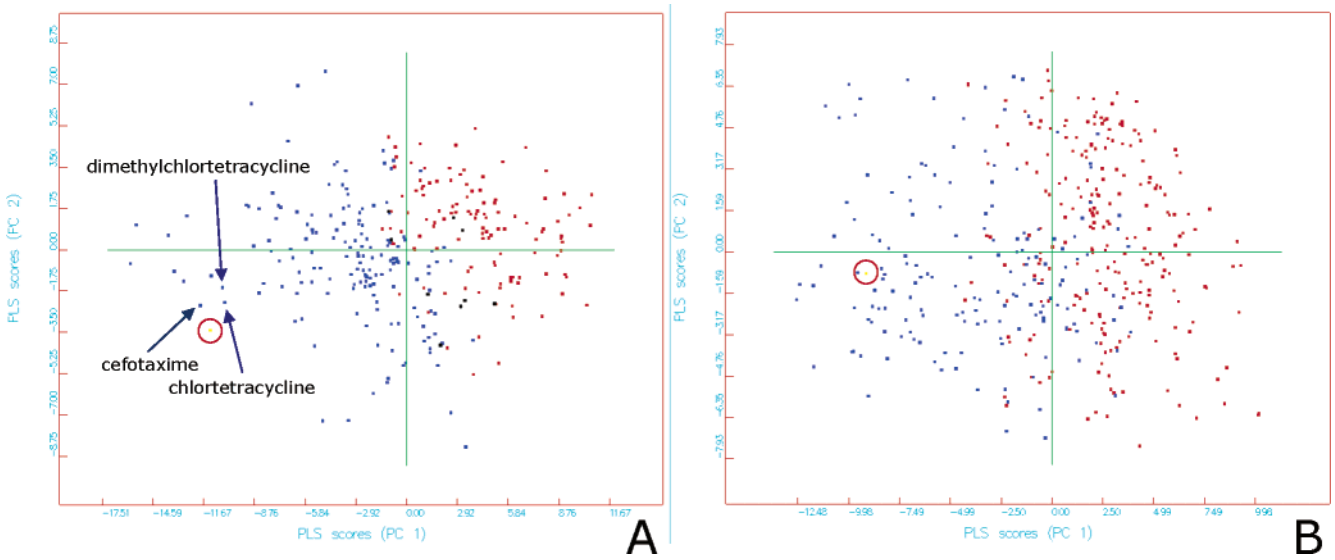

Figure 5. (A) Projection of BBB PLS scores of **8d** (red circle) on BBB PLS scores of compounds with known BBB properties (red, high permeability; blue, low permeability). (B) Projection of Caco2 PLS scores of **8d** (red circle) on Caco2 PLS scores of compounds with known Caco2 properties (red, high permeability; blue, low permeability).

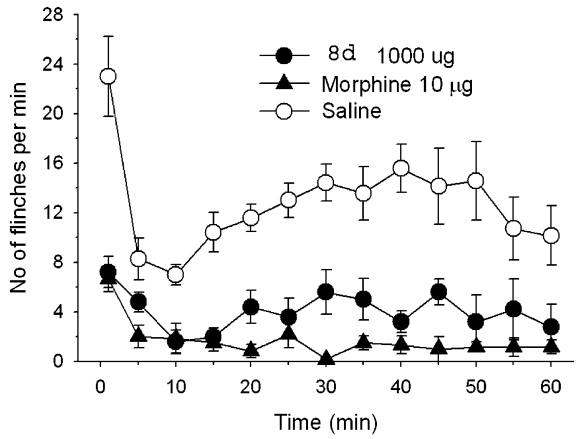

Figure 6. Biphasic pain responses following footpad injection of formalin in the rat. Phase 1 (0−10 min) and phase II (10−60 min) responses were assayed for 1 min at 5 min intervals. **8d** and morphine were administered 10 min before formalin injection. Each point represents the mean ± SEM for five (**8d**) or six (morphine) rats. **8d** reduced phase 1 and phase 2 flinching behavior at $p < 0.05$ by one-way ANOVA. Saline versus **8d** or morphine (phase 1, $p < 0.01$; phase 2, $p < 0.001$; by one-way ANOVA). An amount of 10 μg of morphine is significantly different in phase II from the amount of **8d** ($p < 0.05$ by one-way ANOVA). There is no difference in the phase I response for these two compounds.

0.01; phase 2, $p < 0.001$; by one-way ANOVA). There was no difference between the phase 1 dose−response curve and the phase 2 dose−response curve in **8d** treated rats ($p > 0.6$, by two-way ANOVA). A maximal dose of morphine (10 μg) applied in the same experimental paradigm provided no significant increase in analgesia in comparison to **8d** during phase 1 of this pain study and modestly greater analgesia than **8d** during phase II ($p < 0.05$ by one-way ANOVA). **8d** reduced phase 1 and phase 2 flinching behavior in a dose-dependent manner at doses between 10 and 1000 μg ($p < 0.05$ for both phases between 10 and 1000 mg). While the inflammatory pain model can be affected by both central and peripheral drug actions, the efficacy of **8d** by intrathecal injection clearly supports the conclusion that the drug was acting directly in the spinal cord rather than the periphery. To confirm this, 1000 μg of **8d** was injected peripherally without effect in this pain model. Further, the data in Figure 6 as well as the dose−response data indicate that **8d** was comparably effective in the two distinct phases of the inflammatory pain response.

Conclusions

A series of urea-based compounds have been synthesized and screened for their inhibitory activity in vitro against expressed human GCPII. Several conclusions can be drawn from these studies: (1) the active site of GCPII comprises two regions, namely, the pharmacophore subpocket and the nonpharmacophore subpocket; (2) the pharmacophore subpocket is very sensitive to structural changes, and it is important to keep one of the glutamate moieties intact to maintain the potency of the GCPII inhibitors; (3) the active site within the nonpharmacophore subpocket that binds to glutamate's α-carboxyl group is sensitive to structural change, as shown by compound **7b**; (4) the other active site of the nonpharmacophore subpocket can accommodate both hydrophobic and hydrophilic groups. Importantly, an aromatic ring can be introduced into the inhibitor, thereby increasing its hydrophobicity and thus potentially its ability to cross the blood−brain barrier. Among the compounds tested, compounds **7d**, **8a**, and **8d** show an inhibitory activity in vitro that is comparable or even slightly superior to that of the reported inhibitor, 2-PMPA (**1**). In vivo, intrathecal administration of **8d** also mimics the effects of 2-PMPA and morphine in reducing the response to inflammatory pain evoked by footpad injection of formalin,[9a] thus further supporting the development of GCPII inhibitors for therapeutic purposes. In light of our findings that these compounds significantly interact with GCPII/PSMA, the exploration of the present class of ligands for use in prostate tumor therapy and diagnosis is also underway.[17]

Experimental Section

VolSurf Calculations. VolSurf Caco2 and BBB properties of **8d** were calculated using precalculated Caco2 and BBB models in VolSurf.[16] Compound **8d** was projected on the plot

with the compounds with known Caco2 and BBB properties for comparison. The following parameters were used for the VolSurf setup: Caco2 model contained 396 compounds, BBB model contained 297 compounds, prediction type was set to PLS, and two first principal components (PC 1 and 2) were used to create plots.

General Methods. CH_2Cl_2 was distilled from calcium hydride. ^1H and ^{13}C NMR spectra were acquired at a proton frequency of 300 MHz, using $CDCl_3$ as the solvent unless noted otherwise. ^1H chemical shifts (parts per million, ppm) were obtained using $CHCl_3$ ($\delta = 7.26$, for $CDCl_3$ as the solvent) or HDO ($\delta = 4.80$, for D_2O as the solvent) as the internal standard. ^{13}C chemical shifts (ppm) were determined with $CHCl_3$ (central peak $\delta = 77.00$, for $CDCl_3$ as the solvent) or MeOH ($\delta = 49.15$, for D_2O as the solvent) as the internal standard. TLC was performed on Merck silica gel $60F_{254}$ glass plates. Optical rotations were measured at room temperature.

(*S*)-2-[(*tert*-Butoxycarbonyl)amino]-4-[1-(2-cyanoethyl)-1*H*-tetrazol-5-yl]butyric Acid Benzyl Ester (14). (a) Amide Formation (Method A). To a stirred solution of 3-aminopropionitrile fumarate (1.10 g, 8.59 mmol) in DMF (30 mL) was added *N*-Boc-glutamic acid α-benzyl ester (**12**) (2.31 g, 6.85 mmol) followed by BOP reagent (benzotriazol-1-yloxytris-(dimethylamino)phosphonium hexafluorophosphate; 3.50 g, 7.94 mmol). The reaction mixture was cooled to 0 °C with an ice bath, and then Et_3N (2.20 mL, 15.8 mmol) was added. After being stirred overnight at ambient temperature, the reaction mixture was poured into ice-cold water and extracted with EtOAc. The combined organic layers were washed successively with 1 N HCl, H_2O, saturated $NaHCO_3$, and brine, dried over Na_2SO_4, filtered, and concentrated. The residue was purified by column chromatography (SiO_2, 1:4 EtOAc/hexane) to afford the carboxamide intermediate **13** (1.60 g, 60%).

(b) Tetrazole Formation (Method B). To a stirred suspension of **13** (1.60 g, 4.11 mmol) and Ph_3P (2.82 g, 10.8 mmol) in ice-cold anhydrous CH_3CN (45 mL) were added diisopropyl azodicarboxylate (DIAD) (2.20 mL, 11.2 mmol) and, 2 min later, trimethylsilyl azide (1.60 mL, 11.8 mmol) over 5 min. The heterogeneous reaction mixture was allowed to warm to ambient temperature and then stirred overnight. To the mixture cooled to 0 °C was added a solution of $NaNO_2$ (0.31 g, 4.5 mmol) in H_2O (1.5 mL). After 30 min, a solution of ceric ammonium nitrate (2.50 g, 4.50 mmol) in H_2O (7.0 mL) was added, and the mixture was stirred for 20 min. The mixture was poured into cold water and extracted with CH_2Cl_2. The combined organic layers were washed with H_2O, dried over Na_2SO_4, and concentrated in vacuo. The residue was purified by column chromatography (SiO_2, 1:10 MeOH/$CHCl_3$) to afford **14** (1.05 g, 62%). ^1H NMR δ 7.39 (s, 5H), 5.33 (d, 1H, $J = 6.0$ Hz), 5.21, 5.15 (ABq, 2H, $J = 12.3$ Hz), 4.47 (t, 2H, $J = 6.9$ Hz), 4.37 (m, 1H), 3.05 (t, 2H, $J = 6.9$ Hz), 3.00−2.93 (m, 2H), 2.57 (m, 1H), 2.27 (m, 1H), 1.44 (s, 9H); ^{13}C NMR δ 171.49, 155.56, 154.43, 134.99, 128.61, 128.54, 128.40, 115.90, 80.28, 67.42, 52.72, 42.23, 29.84, 28.17, 19.45, 18.46.

Representative Procedure for the Synthesis of Symmetrical Ureas (Method C): (*S*,*S*)-4,4′-Bis[1-(2-cyanoethyl)-1*H*-tetrazol-5-yl]-2,2′-ureylenedibutyric Acid Dibenzyl Ester (15). To a stirred solution of **14** (205 mg, 0.50 mmol) in dry CH_2Cl_2 (3.0 mL) was added CF_3COOH (1.5 mL). After being stirred at ambient temperature for 3 h, the reaction mixture was poured into CH_2Cl_2 (20 mL) and washed successively with saturated $NaHCO_3$ and H_2O. The organic layer was dried over Na_2SO_4 and concentrated to afford the crude free amine (145 mg, 92%).

To a stirred solution of the above free amine (145 mg, 0.46 mmol) in CH_2Cl_2 (5 mL) at −78 °C were added Et_3N (64 μL, 0.46 mmol) and triphosgene (22.9 mg, 0.23 mmol) in CH_2Cl_2 (0.50 mL). The reaction mixture was then allowed to warm to room temperature, stirred for an additional 2 h, diluted with CH_2Cl_2, washed with H_2O, and dried over Na_2SO_4. Filtration, concentration, and column chromatography (SiO_2, 1:10 MeOH/$CHCl_3$) afforded **15** (70 mg, 47%). ^1H NMR δ 7.34−7.29 (m, 10H), 6.23 (d, 2H, $J = 8.1$ Hz), 5.12 (t, 4H, $J = 12.9$ Hz), 4.59−4.48 (m, 2H), 4.47−4.36 (m, 4H), 2.95−2.89 (m, 8H), 2.56−2.47 (m, 2H), 2.28−2.18 (m, 2H); ^{13}C NMR δ 172.33, 157.64, 154.92, 135.20, 128.64, 128.45, 128.04, 116.61, 67.32, 52.44, 42.25, 29.27, 19.43, 18.33.

Representative Procedure for Benzyl Ester Hydrogenolysis (Method D): (*S*,*S*)-4,4′-Bis[1-(2-cyanoethyl)-1*H*-tetrazol-5-yl]-2,2′-ureylenedibutyric Acid (6c). To a solution of **15** (11 mg, 0.17 mmol) in *tert*-butyl alcohol (5 mL) was added 11 mg of 20% $Pd(OH)_2/C$ (Aldrich, ≤50% H_2O), and the mixture was stirred under 1 atm of H_2 for 1 h. The catalyst was removed by filtration through Celite, and the filtrate was concentrated. The residue was dissolved in 5 mL of water and lyophilized to afford product **6c** (8 mg). $[\alpha]_D$ +5.5° (*c* 0.22, MeOH); ^1H NMR (D_2O) δ 4.72 (t, 4H, $J = 6.3$ Hz), 4.29 (dd, 2H, $J = 4.8$, 9.6 Hz), 3.19 (t, 4H, $J = 6.3$ Hz), 3.10 (t, 4H, $J = 7.2$ Hz), 2.56−2.41 (m, 2H), 2.28−2.16 (m, 2H); ^{13}C NMR (D_2O) δ 176.23, 159.40, 156.08, 118.42, 52.75, 42.82, 28.44, 19.49, 18.21.

Representative Procedure for the Removal of the 2-Cyanoethyl Group (Method E): (*S*,*S*)-4,4′-Di-(1*H*-tetrazol-5-yl)-2,2′-ureylenedibutyric Acid (6d). To a solution of **6c** (8 mg) in CH_2Cl_2 (3 mL) was added DBU (0.1 mL). The reaction mixture was stirred at room temperature for 2 h and then concentrated in vacuo. Filtration over a Dowex-50WX8-400 column (H^+ form; water as the eluent) afforded the product **6d** (4 mg) after lyophilization. $[\alpha]_D$ +12.0° (*c* 0.60, MeOH); ^1H NMR (D_2O) δ 4.24−4.19 (m, 2H), 3.10 (t, 4H, $J = 7.2$ Hz), 2.24−2.32 (m, 2H), 2.23−2.10 (m, 2H); ^{13}C NMR (D_2O) δ 176.48, 159.34, 156.33, 52.97, 28.96, 19.71.

Representative Procedure for the Synthesis of Unsymmetrical Ureas (Method F): (*S*)-2-[3-[(*S*)-1-(Benzyloxycarbonyl)-3-[1-(2-cyanoethyl)-1*H*-tetrazol-5-yl]propyl]ureido]pentanedioic Acid Dibenzyl Ester (16). To a stirred solution tosylate of dibenzyl glutamate (250 mg, 0.50 mmol) and triphosgene (50 mg, 0.17 mmol) in CH_2Cl_2 (5 mL) at −78 °C were added Et_3N (0.23 mL, 1.64 mmol) in CH_2Cl_2 (1.0 mL). The reaction mixture was allowed to warm to room temperature to afford isocyanate **11**. Then the free amine, obtained from compound **14** (127 mg, 0.30 mmol) as before, was added to the isocyanate solution, and the mixture was stirred overnight. The reaction mixture was diluted with CH_2Cl_2, washed with H_2O, and dried over Na_2SO_4. Filtration, concentration, and column chromatography (SiO_2, 1:20 MeOH/$CHCl_3$) afforded **16** (85 mg, 43%). ^1H NMR ($CDCl_3$) δ 7.35−7.24 (m, 15H), 5.83−5.79 (m, 2H), 5.13 (s, 2H), 5.09 (s, 2H), 5.05 (s, 2H), 4.59−4.27 (m, 4H), 2.91−2.83 (m, 4H), 2.80−2.36 (m, 3H), 2.15 (m, 1H), 2.04−1.88 (m, 2H). ^{13}C NMR ($CDCl_3$) δ 172.99, 172.74, 172.11, 157.26, 154.81, 135.61, 135.29, 135.03, 128.59, 128.51, 128.47, 128.36, 128.24, 128.11, 127.86, 116.38, 67.40, 67.14, 66.47, 52.68, 52.24, 42.14, 30.32, 30.04, 27.16, 19.28, 18.35.

(2*S*,2′*S*,4*R*,4′*R*)-*N*,*N*′-Carbonyl-4,4′-dimethyldiglutamic Acid Tetrabenzyl Ester (10a). 10a was synthesized from **9a** according to method C. ^1H NMR δ 7.34−7.27 (m, 20H), 5.15−5.03 (m, 10H), 4.60−4.53 (m, 2H), 2.63−2.52 (m, 2H), 2.28−2.17 (m, 2H), 1.76−1.66 (m, 2H), 1.15 (d, 6H, $J = 7.2$ Hz); ^{13}C NMR δ 175.61, 172.74, 156.36, 135.96, 135.29, 128.53, 128.50, 128.31, 128.13, 128.08, 128.03, 67.05, 66.33, 51.61, 36.14, 17.47.

(2*S*,2′*S*,4*R*,4′*R*)-*N*,*N*′-Carbonyl-4,4′-dimethyldiglutamic Acid (5a). 5a was synthesized from **10a** according to method D. $[\alpha]_D$ +2.3° (*c* 0.17, MeOH); ^1H NMR (D_2O) δ 4.37 (dd, 2H, $J = 4.5$, 9.9 Hz), 2.73−2.59 (m, 2H), 2.24−2.15 (m, 2H), 1.86−1.76 (m, 2H), 1.20 (d, 6H, $J = 7.2$ Hz); ^{13}C NMR (D_2O) δ 180.74, 176.84, 159.22, 51.99, 36.47, 34.88, 17.20.

(2*S*,2′*S*,4*R*,4′*R*)-4,4′-Dibenzyl-*N*,*N*′-carbonyldiglutamic Acid Tetrabenzyl Ester (10b). 10b was synthesized from **9b** according to method C. ^1H NMR δ 7.30−6.94 (m, 30H), 5.06−4.93 (m, 10H), 4.59−4.52 (m, 2H), 2.91−2.64 (m, 6H), 2.25−2.16 (m, 2H), 1.75−1.66 (m, 2H); ^{13}C NMR δ 174.37, 172.53, 156.26, 138.23, 135.74, 135.21, 128.92, 128.49, 128.34, 128.24, 128.10, 128.08, 127.96, 126.42, 67.00, 66.33, 51.56, 43.58, 38.33, 34.13.

(2*S*,2′*S*,4*R*,4′*R*)-4,4′-Dibenzyl-*N*,*N*′-carbonyldiglutamic Acid (5b). 5b was synthesized from **10b** according to

method D. $[\alpha]_D$ +11.7° (*c* 0.33, MeOH); ^{1}H NMR (D_2O) δ 7.26−7.15 (m, 10H), 4.32−4.28 (m, 2H), 2.98−2.75 (m, 6H), 2.20−2.11 (m, 2H), 1.72−1.61 (m, 2H); ^{13}C NMR (D_2O) δ 178.49, 176.32, 160.30, 140.39, 130.30, 129.57, 127.60, 53.00, 45.41, 39.78, 35.75.

(2*S*,2′*S*,4*S*,4′*S*)-*N*,*N*′-Carbonyl-4,4′-dimethyldiglutamic Acid Tetrabenzyl Ester (10c). 10c was synthesized from **9c** according to method C. ^{1}H NMR δ 7.36−7.26 (m, 20H), 5.14−4.98 (m, 10H), 4.55 (dt, 2H, J = 4.8, 13.2 Hz), 2.65−2.54 (m, 2H), 2.10−2.00 (m, 2H), 1.93−1.85 (m, 2H), 1.19 (d, 6H, J = 6.9 Hz); ^{13}C NMR δ 176.06, 172.75, 156.70, 135.89, 135.22, 128.56, 128.54, 128.37, 128.20, 128.11, 67.19, 66.42, 51.54, 36.32, 35.92, 17.11.

(2*S*,2′*S*,4*S*,4′*S*)-*N*,*N*′-Carbonyl-4,4′-dimethyldiglutamic Acid (5c). 5c was synthesized from **10c** according to method D. $[\alpha]_D$ +8.0° (*c* 0.21, MeOH); ^{1}H NMR (D_2O) δ 4.27 (dd, 2H, J = 4.8, 9.6 Hz), 2.60 (dt, 2H, J = 6.6, 21.0 Hz), 2.11−1.90 (m, 4H), 1.18 (d, 6H, J = 6.6 Hz); ^{13}C NMR (D_2O) δ 181.17, 176.98, 159.39, 51.93, 36.69, 34.73, 16.40.

(*S*,*S*)-*N*,*N*′-Carbonyl-2,2′-dimethyldiglutamic Acid Tetrabenzyl Ester (10d). 10d was synthesized from **9d** according to method C. ^{1}H NMR δ 7.32−7.30 (m, 20H), 5.33 (s, 2H), 5.13−5.06 (m, 8H), 2.46−2.16 (m, 8H), 1.53 (s, 6H); ^{13}C NMR δ 174.28, 172.96, 155.24, 135.75, 135.50, 128.48, 128.45, 128.20, 128.16, 128.12, 128.08, 67.24, 66.30, 59.00, 32.11, 29.21, 23.53.

(*S*,*S*)-*N*,*N*′-Carbonyl-2,2′-dimethyldiglutamic Acid (5d). 5d was synthesized from **10d** according to method D. $[\alpha]_D$ +5.2° (*c* 0.57, MeOH); ^{1}H NMR (D_2O) δ 2.43−2.20 (m, 6H), 2.12−2.02 (m, 2H), 1.41 (s, 6H); ^{13}C NMR (D_2O) δ 178.57, 178.03, 157.56, 58.06, 31.46, 28.81, 22.70.

(2*S*,2′*S*,4*R*)-4-Benzyl-*N*,*N*′-carbonyldiglutamic Acid Tetrabenzyl Ester (10e). 10e was synthesized from **5b** and isocyanate **11**. ^{1}H NMR δ 7.36−6.99 (m, 25H), 5.16−4.98 (m, 10H), 4.63−4.49 (m, 2H), 2.93 (m, 1H), 2.84−2.67 (m, 2H), 2.47−2.10 (m, 4H), 1.93 (m, 1H), 1.77 (m, 1H); ^{13}C NMR δ 174.43, 172.71, 172.59, 172.49, 156.42, 138.22, 135.73, 135.19, 128.95, 128.55, 128.53, 128.49, 128.42, 128.40, 128.36, 128.30, 128.16, 128.04, 126.47, 67.16, 67.09, 66.40, 66.38, 52.40, 51.70, 43.62, 38.33, 33.98, 30.16, 27.97.

(2*S*,2′*S*,4*R*)-4-Benzyl-*N*,*N*′-carbonyldiglutamic Acid (5e). 5e was synthesized from **10e** according to method D. $[\alpha]_D$ −3.2° (*c* 0.22, MeOH); ^{1}H NMR (D_2O) δ 7.39−7.26 (m, 5H), 4.25−4.18 (m, 2H), 3.00−2.87 (m, 3H), 2.49 (t, 2H, J = 7.2 Hz), 2.27−2.10 (m, 2H), 2.01−1.83 (m, 2H); ^{13}C NMR (D_2O) δ 179.26, 177.64, 176.80, 176.67, 159.22, 138.74, 129.20, 128.83, 126.96, 52.96, 52.09, 44.52, 38.25, 33.07, 30.29, 26.64.

(2*S*,2′*S*,4*S*)-*N*,*N*′-Carbonyl-4-methyldiglutamic Acid Tetrabenzyl Ester (10f). 10f was synthesized from **5c** and isocyanate **11**. ^{1}H NMR δ 7.33−7.31 (m, 20H), 5.18−4.96 (m, 10H), 4.59−4.50 (m, 2H), 2.60 (m, 1H), 2.49−2.31 (m, 2H), 2.24−1.85 (m, 4H), 1.20 (d, 3H, J = 6.9 Hz); ^{13}C NMR δ 176.08, 172.79, 172.73, 172.39, 156.59, 135.87, 135.75, 135.20, 135.17, 128.57, 128.54, 128.42, 128.39, 128.21, 128.09, 67.24, 67.22, 66.44, 66.43, 52.53, 51.62, 36.38, 35.92, 30.20, 27.88, 17.14.

(2*S*,2′*S*,4*S*)-*N*,*N*′-Carbonyl-4-methyldiglutamic Acid (5f). 5f was synthesized from **10f** according to method D. $[\alpha]_D$ +18.0° (*c* 0.16, MeOH); ^{1}H NMR (D_2O) δ 4.17−4.09 (m, 2H), 2.48 (m, 1H), 2.37 (t, 2H, J = 7.5 Hz), 2.10−1.78 (m, 4H), 1.06 (d, 3H, J = 7.2 Hz); ^{13}C NMR (D_2O) δ 181.13, 177.57, 176.91, 176.67, 159.34, 52.90, 51.89, 36.71, 34.64, 30.26, 26.50, 16.42.

(*S*)-4-(Benzylcarbamoyl)-2-[(*tert*-butoxycarbonyl)-amino]butyric Acid Benzyl Ester (17). 17 was synthesized from **12** and benzylamine according to method A. ^{1}H NMR δ 7.29−7.17 (m, 10H), 6.97 (br, 1H), 5.68 (d, 1H, J = 8.1 Hz), 5.11, 5.04 (ABq, 2H, J = 12.3 Hz), 4.30 (d, 2H, J = 5.4 Hz), 4.25 (m, 1H), 2.32 (t, 2H, J = 7.2 Hz), 2.11 (m, 1H), 1.94 (m, 1H), 1.39 (s, 9H); ^{13}C NMR δ 172.09, 171.92, 155.60, 137.90, 135.04, 128.27, 128.10, 127.94, 127.33, 127.27, 127.02, 79.64, 66.74, 53.02, 43.19, 31.94, 27.98.

(*S*)-4-(1-Benzyl-1*H*-tetrazol-5-yl)-2-[(*tert*-butoxycarbonyl)amino]butyric Acid Benzyl Ester (18). 18 was synthesized from **17** according to method B. ^{1}H NMR δ 7.37−7.12 (m, 10H), 5.44, 5.38 (ABq, 2H, J = 15.6 Hz), 5.21 (m, 1H), 5.11 (s, 2H), 4.34 (m, 1H), 2.84−2.66 (m, 2H), 2.30 (m, 1H), 2.05 (m, 1H), 1.41 (s, 9H); ^{13}C NMR δ 171.48, 154.00, 134.96, 133.10, 129.20, 128.92, 128.61, 128.56, 128.37, 127.48, 79.95, 67.40, 52.83, 50.67, 29.77, 28.20, 19.81.

(*S*,*S*)-4,4′-Bis(1-benzyl-1*H*-tetrazol-5-yl)-2,2′-ureylenedibutyric Acid Dibenzyl Ester (19). 19 was synthesized from **18** according to method C. ^{1}H NMR δ 7.30−7.12 (m, 20H), 6.36 (d, 2H, J = 8.4 Hz), 5.39, 5.33 (AB, 4H, J = 15.6 Hz), 5.04 (s, 4H), 4.58−4.51 (m, 2H), 2.89−2.72 (m, 4H), 2.35−2.24 (m, 2H), 2.17−2.05 (m, 2H); ^{13}C NMR δ 172.11, 157.45, 154.38, 135.09, 133.14, 129.05, 128.74, 128.47, 128.30, 128.02, 127.64, 67.06, 52.47, 50.55, 29.39, 19.79.

(*S*)-4-[(*tert*-Butoxycarbonyl)amino]-4-[1-(2-cyanoethyl)-1*H*-tetrazol-5-yl]butyric Acid Benzyl Ester. This compound was prepared from *N*-Boc-glutamic acid α-benzyl ester and 3-aminopropionitrile fumarate according to methods A and B. ^{1}H NMR δ 7.35 (s, 5H), 5.71 (d, 1H, J = 8.1 Hz), 5.19, 5.14 (AB, 1H, J = 7.5 Hz), 5.11 (s, 2H), 4.80−4.64 (m, 2H), 3.06 (t, 2H, J = 6.9 Hz), 2.70−2.43 (m, 2H), 2.37−2.30 (m, 2H); ^{13}C NMR δ 172.28, 155.61, 155.29, 135.37, 128.42, 128.18, 128.10, 115.91, 80.68, 66.47, 43.27, 42.45, 29.77, 28.31, 27.98, 18.21.

(*S*,*S*)-4,4′-Bis[1-(2-cyanoethyl)-1*H*-tetrazol-5-yl]-4,4′-ureylenedibutyric Acid Dibenzyl Ester. This compound was prepared from the preceding intermediate according to method C. ^{1}H NMR δ 7.40−7.25 (m, 10H), 6.52 (d, 2H, J = 8.1 Hz), 5.29−5.21 (m, 2H), 5.08, 5.03 (AB, 4H, J = 12.3 Hz), 4.76−4.60 (m, 4H), 3.02 (t, 4H, J = 6.9 Hz), 2.25−2.20 (m, 8H); ^{13}C NMR δ 172.48, 156.70, 156.17, 135.51, 128.68, 128.49, 128.36, 116.01, 66.75, 42.90, 42.73, 30.01, 28.76, 18.41.

(*S*,*S*)-4,4′-Bis[1-(2-cyanoethyl)-1*H*-tetrazol-5-yl]-4,4′-ureylenedibutyric Acid (6a). 6a was prepared from the preceding intermediate according to method D. $[\alpha]_D$ −31.2° (*c* 0.67, MeOH); ^{1}H NMR (D_2O) δ 5.22 (t, 2H, J = 7.2 Hz), 4.82−4.77 (m, 4H), 3.25 (t, 4H, J = 6.6 Hz), 2.49 (t, 4H, J = 6.9 Hz), 2.31−2.24 (m, 4H); ^{13}C NMR (D_2O) δ 177.19, 158.04, 156.75, 118.10, 43.63, 43.16, 30.02, 27.71, 18.00.

(*S*,*S*)-4,4′-Di-(1*H*-tetrazol-5-yl)-4,4′-ureylenedibutyric Acid (6b). 6b was synthesized from **6a** according to method E. $[\alpha]_D$ −26.0° (*c* 0.10, MeOH); ^{1}H NMR (D_2O) δ 5.16 (dd, 2H, J = 6.0, 9.0 Hz), 2.52 (t, 4H, J = 6.9 Hz), 2.38−2.29 (m, 4H); ^{13}C NMR (D_2O) δ 177.10, 158.58, 158.37, 45.22, 29.94, 27.97.

(*S*)-2-[3-[(*S*)-3-(Benzyloxycarbonyl)-1-[1-(2-cyanoethyl)-1*H*-tetrazol-5-yl]propyl]ureido]pentanedioic Acid Dibenzyl Ester. This compound was prepared from (*S*)-4-[(*tert*-butoxycarbonyl)amino]-4-[1-(2-cyanoethyl)-1*H*-tetrazol-5-yl]butyric acid benzyl ester and isocyanate **11**. ^{1}H NMR δ 7.37−7.26 (m, 15H), 6.35 (d, 1H, J = 9.0 Hz), 5.98 (d, 1H, J = 7.8 Hz), 5.36, 5.31 (AB, 1H, J = 8.1 Hz), 5.18−5.08 (m, 4H), 5.00 (s, 2H), 4.80−4.58 (m, 2H), 4.45 (m, 1H), 2.95 (t, 2H, J = 6.6 Hz), 2.61−1.90 (m, 8H); ^{13}C NMR δ 172.61, 172.53, 172.29, 156.79, 156.38, 135.69, 135.52, 135.20, 128.57, 128.55, 128.53, 128.39, 128.33, 128.28, 128.24, 128.13, 115.97, 67.18, 66.71, 66.36, 52.69, 42.70, 42.55, 30.13, 29.99, 28.92, 27.31, 18.34.

(*S*)-2-[3-[(*S*)-3-Carboxy-1-[1-(2-cyanoethyl)-1*H*-tetrazol-5-yl]propyl]ureido]pentanedioic Acid (7a). 7a was prepared from the preceding intermediate according to method D. $[\alpha]_D$ +10.4° (*c* 0.25, MeOH); ^{1}H NMR (D_2O) δ 5.25 (dd, 1H, J = 6.6, 8.1 Hz), 4.82−4.77 (m, 2H), 4.16 (dd, 1H, J = 5.1, 9.3 Hz), 3.24 (t, 2H, J = 6.6 Hz), 2.62−2.49 (m, 6H), 2.14 (m, 1H), 1.92 (m, 1H); ^{13}C NMR (D_2O) δ 177.94, 177.52, 177.50, 158.82, 156.97, 118.23, 53.77, 43.72, 43.29, 30.64, 30.25, 27.95, 26.92, 18.14.

(*S*)-2-[3-[(*S*)-3-Carboxy-1-(1*H*-tetrazol-5-yl)propyl]-ureido]pentanedioic Acid (7b). 7b was synthesized from **7a** according to method E. $[\alpha]_D$ −18.8° (*c* 0.46, MeOH); ^{1}H NMR (D_2O) δ 5.18 (dd, 1H, J = 5.4, 9.0 Hz), 4.22 (dd, 1H, J = 5.1, 9.0 Hz), 2.57−2.46 (m, 4H), 2.39−2.11 (m, 3H), 1.98 (m, 1H); ^{13}C NMR (D_2O) δ 177.69, 177.29, 176.66, 159.15, 158.65, 53.06, 45.33, 30.43, 30.09, 28.19, 26.46.

(*S*)-2-[3-[(*S*)-1-Carboxy-3-[1-(2-cyanoethyl)-1*H*-tetrazol-5-yl]propyl]ureido]pentanedioic Acid (7c). 7c was synthesized from **16** according to method D. $[\alpha]_D$ +3.7° (*c* 0.21, MeOH); ^{1}H NMR (D_2O) δ 4.72 (t, 2H, J = 6.3 Hz), 4.31 (m, 1H), 4.24 (m, 1H), 3.19 (t, 2H, J = 6.3 Hz), 3.10 (t, 2H, J = 7.5

Hz), 2.52−2.42 (m, 3H), 2.28−2.11 (m, 2H), 1.97 (m, 1H); ^{13}C NMR (D_2O) δ 177.63, 176.68, 176.19, 159.48, 156.07, 118.41, 52.97, 52.68, 42.81, 30.40, 28.48, 26.51, 19.46, 18.20..

(*S*)-2-[3-[(*S*)-1-Carboxy-3-(1*H*-tetrazol-5-yl)propyl]-ureido]pentanedioic Acid (7d). 7d was synthesized from **7c** according to method E. $[\alpha]_D$ −18.8° (*c* 0.46, MeOH); ^{1}H NMR (D_2O) δ 5.18 (dd, 1H, J = 5.4, 9.0 Hz), 4.22 (dd, 1H, J = 5.1, 9.0 Hz), 2.57−2.46 (m, 4H), 2.39−2.11 (m, 3H), 1.98 (m, 1H); ^{13}C NMR (D_2O) δ 177.69, 177.29, 176.66, 159.15, 158.65, 53.06, 45.33, 30.43, 30.09, 28.19, 26.46.

(*S*)-2-[3-((*S*)-α-Carboxybenzyl)ureido]pentanedioic Acid (8a). 8a was prepared from isocyanate **11** and L-phenylglycine followed by hydrogenation. $[\alpha]_D$ +62.9° (*c* 0.41, MeOH); ^{1}H NMR (D_2O) δ 7.43 (m, 5H), 5.24 (s, 1H), 4.25 (dd, 1H, J = 5.1, 9.0 Hz), 2.47 (t, 2H, J = 7.2 Hz), 2.17 (m, 1H), 1.95 (m, 1H); ^{13}C NMR (D_2O) δ 177.59, 176.67, 175.5, 158.96, 137.10, 129.30, 128.80, 127.41, 58.41, 52.88, 30.25, 26.55.

(*S*)-2-[3-[(*S*)-1-(Benzyloxycarbonyl)-2-phenylethyl]-ureido]pentanedioic Acid Dibenzyl Ester (21b). 21b was synthesized from **20b** and isocyanate **11**. ^{1}H NMR δ 7.36−6.94 (m, 20H), 5.35−4.98 (m, 8H), 4.82 (m, 1H), 4.57 (m, 1H), 3.10−2.98 (m, 2H), 2.47−2.29 (m, 2H), 2.16 (m, 1H), 1.90 (m, 1H); ^{13}C NMR δ 172.85, 172.70, 172.16, 156.31, 135.79, 135.74, 135.19, 129.45, 128.54, 128.51, 128.41, 128.20, 128.18, 126.91, 67.28, 67.11, 66.42, 53.91, 52.42, 38.49, 30.24, 27.91.

(*S*)-2-[3-((S)-1-Carboxy-2-phenylethyl)ureido]pentanedioic Acid (8b). 8b was synthesized from **21b** according to method D. $[\alpha]_D$ +40.2° (*c* 0.18, MeOH); ^{1}H NMR (D_2O) δ 7.42−7.24 (m, 5H), 4.47 (m, 1H), 4.15 (m, 1H), 3.19 (m, 1H), 3.02 (m, 1H), 2.48−2.40 (m, 2H), 2.11 (m, 1H), 1.90 (m, 1H); ^{13}C NMR (D_2O) δ 177.69, 176.88, 159.07, 137.02, 129.50, 128.82, 127.19, 55.18, 53.03, 37.52, 30.33, 26.64.

(*S*)-2-[3-[(*S*)-α-(Benzyloxycarbonyl)-4-hydroxybenzyl]-ureido]pentanedioic Acid Dibenzyl Ester (21c). 21c was synthesized from **20c** and isocyanate **11**. ^{1}H NMR ($CDCl_3$) δ 7.37−7.16 (m, 15H), 7.09 (d, 2H. J = 8.7 Hz), 6.58 (d, 2H, J = 8.7 Hz), 6.21 (br, 1H), 5.79 (br, 1H), 5.42−5.38 (m, 2H), 5.16−5.05 (m, 6H), 4.54 (m, 1H), 2.48−2.30 (m, 2H), 2.16 (m, 1H), 1.96 (m, 1H).

(*S*)-2-[3-((*S*)-α-Carboxy-4-hydroxybenzyl)ureido]pentanedioic Acid (8c). 8c was synthesized from **21c** according to method D. $[\alpha]_D$ +85.7° (*c* 0.64, MeOH); ^{1}H NMR (D_2O) δ 7.29 (d, 2H, J = 8.1 Hz), 6.89 (d, 2H, J = 8.1 Hz), 5.18 (s, 1H), 4.25 (dd, 1H, J = 5.1, 8.7 Hz), 2.46 (t, 2H, J = 6.9 Hz), 2.13 (m, 1H), 1.94 (m, 1H); ^{13}C NMR (D_2O) δ 177.57, 176.52, 175.46, 159.09, 156.20, 129.26, 128.22, 116.18, 57.52, 52.83, 30.29, 26.57.

(*S*)-2-[3-[(*S*)-1-(Benzyloxycarbonyl)-2-(4-hydroxyphenyl)ethyl]ureido]pentanedioic Acid Dibenzyl Ester (21d). 21d was synthesized from **20d** and isocyanate **11**. ^{1}H NMR δ 7.55 (m, 1H), 7.32−7.22 (m, 15H), 6.67 (d, 2H, J = 8.1 Hz), 6.58 (d, 2H, J = 8.1 Hz), 5.88 (m, 1H), 5.65 (m, 1H), 5.14−4.90 (m, 6H), 4.82 (br, 1H), 4.61 (m, 1H), 2.98−2.86 (m, 2H), 2.44−2.25 (m, 2H), 2.11 (m, 1H), 1.81 (m, 1H); ^{13}C NMR δ 173.34, 172.79, 172.31, 156.80, 155.31, 135.58, 135.03, 134.98, 130.54, 128.66, 128.51, 128.48, 128.44, 128.40, 128.36, 128.16, 126.71, 115.42, 67.51, 67.14, 66.46, 53.74, 52.10, 37.52, 30.18, 28.10.

(*S*)-2-[3-[(*S*)-1-Carboxy-2-(4-hydroxyphenyl)ethyl]-ureido]pentanedioic Acid (8d). 8d was synthesized from **21d** according to method D. $[\alpha]_D$ +34.9° (*c* 0.48, MeOH); ^{1}H NMR (D_2O) δ 7.14 (d, 2H, J = 7.2 Hz), 6.83 (d, J = 7.2 Hz), 4.43 (m, 1H), 4.17 (m, 1H), 3.07 (m, 1H), 2.93 (m, 1H), 2.43 (t, 2H, J = 6.9 Hz), 2.11 (m, 1H), 1.90 (m, 1H); ^{13}C NMR (D_2O) δ 177.49, 176.54, 176.48, 159.10, 154.52, 130.81, 128.62, 115.55, 54.99, 52.74, 36.50, 30.17, 26.43.

Biological Assay Methods. The inhibitory activity of all compounds was determined using a fluorescent assay of human GCPII activity. The enzyme used in the assay was obtained from a Chinese hamster ovary (CHO) cell line transfected with the cloned human cDNA for GCPII using the calcium phosphate method, as described previously.[5d] Cells grown to confluency, were harvested in 50 mM Tris-HCl, pH 7.4, and subjected to freezing and thawing. Cell membranes were washed three times by centrifugation, and the final aliquots of membranes were adjusted to a protein concentration of 20 mg/mL and stored at −80 °C. The GPCPII activity was assayed in a two-step process. In the first step, aliquots of membranes (4 μg) were incubated for 2 h at 37 °C in 50 mM Tris-HCl, pH 7.4, in the presence of 4 μM NAAG and the given inhibitor, in a volume of 100 μL, to allow for the accumulation of glutamate produced in the GPCII reaction. In the second step, the amount of accumulated glutamate was measured using the Amplex Red glutamic acid assay kit (Molecular Probes), and the fluorescence was read with a Dynex fluorescent plate reader using excitation at 530 nm and emission at 590 nm. For all inhibitors, dose−response curves were obtained and were used to calculate IC_{50} values by nonlinear regression using the Sigma-Plot software. In each series of experiments a concentration curve of NAAG was used to determine the K_m. The final K_i values for each inhibitor were calculated from the respective IC_{50} and K_m values using the Cheng and Prusoff equation.

Pain Assay Methods. The following investigations were performed according to a protocol approved by the Institutional Animal Care Committee of Chiba University, Chiba, Japan, consistent with international standards for care and use of experimental animals. Male Sprague−Dawley rats weighing 250−300 g were fitted with long-term intrathecal catheters and examined for the effects of ZJ17 on the formalin test.

Intrathecal Catheters. Chronic intrathecal catheters were inserted, during halothane anesthesia, by passing a PE-10 catheter through an incision in the atlanta-occipital membrane to a position 8 cm caudal to the cisterna at the level of lumbar enlargement.[9a,b] The catheter was externalized on the top of the skull and sealed with a steel wire, and the wound was closed with 3-0 silk sutures. The animals were allowed to recover for 1 week before being used experimentally. All animals displayed normal feeding and drinking behavior postoperatively. Rats showing neurological deficits were not studied.

Formalin Test. To carry out the formalin test, the animal was briefly anesthetized with halothane (4%). When there was momentary loss of spontaneous movement with preservation of the deep spontaneous respiration, blink and pinnae reflexes, 50 μL of 5% formalin was injected subcutaneously into the dorsal surface of the right hind paw with a 27-gauge needle. Immediately after the formalin injection, the animal was placed in an open Plexiglas box (10 cm × 20 cm × 24 cm), which permitted observation. Within 1 min after the formalin injection, the rat held its injected pay just off the floor, a behavior typical of this model. During this period, spontaneous flinching of the injected paw could also be observed. Flinching is readily discriminated and is characterized as a rapid and brief withdrawal or flexion of the injected paw. This pain-related behavior was quantified by counting the number of flinches for 1 min periods at 1−2 and 5−6 min and then for 1 min periods at 5 min intervals during the period from 10 to 60 min after the injection. Two phases of spontaneous flinching behavior were observed. An initial acute phase (phase 1, during the first 6 min after the formalin injection) was followed by a relatively short quiescent period and then by a prolonged tonic response (phase 2, beginning about 10 min after the formalin injection). After the observation period, the animals were immediately killed with an overdose of barbiturate.

Acknowledgment. This work was supported by the National Institutes of Health (Grants NS 35449, NS 38080, and NS 42672). We also thank Drs. Werner Tueckmantel and S.-B. Rong for their help in the preparation of this manuscript.

References

(1) Wahlgren, N. G. Neuroprotective agents and cerebral ischemia. *International Review of Neurobiology*; Green, A. R., Cross, A. J., Eds.; Academic Press: San Diego, CA, 1997; pp 337−363.

(2) Neale, J. H.; Bzdega, T.; Wroblewska, B. *N*-Acetylaspartylglutamate: The most abundant peptide neurotransmitter in the mammalian central nervous system. *J. Neurochem*. **2000**, *75*, 443−452.

(3) (a) Wroblewska, B.; Wroblewski, J. T.; Pshenichkin, S.; Surin, A.; Sullivan, S. E.; Neale, J. H. *N*-Acetylaspartylglutamate selectively activates mGluR3 receptors in transfected cells. *J. Neurochem*. **1997**, *69*, 174−182. (b) Wroblewska, B.; Santi, M. R.; Neale, J. H. *N*-Acetylaspartylglutamate activates cyclic-AMP coupled metabotropic glutamate receptors in cerebellar astrocytes. *Glia* **1998**, *24*, 172−180. (c) Wroblewska, B.; Wroblewski, J. T.; Saab, O.; Neale, J. H. *N*-Acetylaspartylglutamate inhibits forskolin-stimulated cyclic AMP levels via a metabotropic glutamate receptor in cultured cerebellar granule cells. *J. Neurochem*. **1993**, *61*, 943−948. (d) Schaffhauser, H.; Richards, J. G.; Cartmell, J.; Chaboz, S.; Kemp, J. A.; Klingelschmidt, A.; Messer, J.; Stadler, H.; Woltering, T.; Mutel, V. In vitro binding characteristics of a new selective group II metabotropic glutamate receptor radioligand, [^{3}H]Ly354740, in rat brain. *Mol. Pharmacol*. **1998**, *53*, 228−233.

(4) (a) Robinson, M. B.; Blakely, R. D.; Couto, R.; Coyle, J. T. Hydrolysis of the brain dipeptide *N*-acetyl-l-aspartyl-L-glutamate. *J. Biol. Chem*. **1987**, *262*, 14498−14506. (b) Serval, V.; Barbeito, L.; Pittaluga, A.; Cheramy, A.; Lavielle, S.; Glowinski, J. Competitive inhibition of *N*-acetylated-α-linked acidic dipeptidase activity by *N*-acetyl-L-aspartyl-*β*-linked L-glutamate. *J. Neurochem*. **1990**, *55*, 39−46. (c) Carter, R. E.; Feldman, A. R.; Coyle, J. T. Prostate-specific membrane antigen is a hydrolase with substrate and pharmacologic characteristics of a neuropeptidase. *Proc. Natl. Acad. Sci. U.S.A*. **1996**, *93*, 749−753. (d) Bzdega, T.; Turi, T.; Wroblewska, B.; She, D.; Chung, H. S.; Kim, H.; Neale, J. H. Molecular cloning of a peptidase against *N*-acetylaspartylglutamate (NAAG) from a rat hippocampal cDNA library. *J. Neurochem*. **1997**, *69*, 2270−2278. (e) Luthi-Carter, R.; Berger, U. V.; Barczak, A. K.; Coyle, J. T. Isolation and expression of rat brain cDNA encoding glutamate carboxypeptidase II. *Proc. Natl. Acad. Sci. U.S.A*. **1988**, *95*, 3215−3220.

(5) (a) Slusher, B. S.; Vornov, J. J.; Thomas, A. G.; Hurn, P. D.; Harukuni, I.; Bhardwaj, A.; Traystman, R. J.; Robinson, M. B.; Britton, P.; Lu, X.-C. M.; Tortella, F. C.; Wozniak, K. M.; Yudkoff, M.; Potter, B. M.; Jackson, P. F. Selective inhibition of NAALADase, which converts NAAG to glutamate, reduces ischemic brain injury. *Nat. Med*. **1999**, *5*, 1396−1402. (b) Tyson, R. L.; Sutherland, G. R. Labeling of *N*-acetylaspartate and *N*-acetylaspartylglluamate in rat neocortex, hippocampus and cerebellum from [1-^{13}C]-glucose. *Neurosci. Lett*. **1998**, *251*, 181−184.

(6) (a) Bruno, V.; Battaglia, G.; Copani, A.; Giffard, R. G.; Raciti, G.; Raffaele, R.; Shinozaki, H.; Nicoletti, F. Activation of class II or III metabotropic glutamate receptors protects cultured cortical neurons against excitotoxic degeneration. *Eur. J. Pharmacol*. **1995**, *7*, 1906−1913. (b) Bruno, V.; Wroblewska, B.; Wroblewski, J. T.; Fiore, L.; Nicoletti, F. Neuroprotective activity of *N*-actylaspartylglutamate in cultured cortical cells. *Neuroscience* **1998**, *85*, 751−757. (c) Jackson, P. F.; Slusher, B. S. Design of NAALADase inhibitors: a novel neuroprotective strategy. *Curr. Med. Chem*. **2001**, *8*, 949−957. (d) Thomas, A. G.; Vornov, J. J.; Olkowski, J. L.; Merion, A. T.; Slusher, B. S. *N*-Acetylated alpha-linked acidic dipeptidase converts *N*-acetylsapartylglutamate from a neuroprotectant to a neurotoxin. *J. Pharmacol. Exp. Ther*. **2000**, *295*, 16−22

(7) (a) Dolan, S.; Nolan, A. M. Behavioral evidence supporting a different role for Group I and II metabotropic glutamate receptors in spinal nociceptive transmission. *Neuropharmacology* **2000**, *39*, 1132−1138. (b) Neugebauer, V. Metabotropic glutamate receptors—important modulators of nociception and pain behavior. *Pain* **2002**, *98*, 1−8.

(8) (a) Jackson, P. F.; Cole, D. C.; Slusher, B. S.; Stetz, S. L.; Ross, L. E.; Donzati, B. A.; Trainor, D. A. Design, synthesis, and biological activity of a potent inhibitor of neuropeptidase *N*-acetylated-α-linked acidic dipeptidase. *J. Med. Chem*. **1996**, *39*, 619−622. (b) Jackson, P. F.; Tays, K. L.; Maclin, K. M.; Ko, Y. S.; Li, W.; Vitharana, D.; Tsukamoto, T.; Stoermer, D.; Lu, X.-C. M.; Wozniak, K.; Slusher, B. S. Design and pharmacological activity of phosphinic acid based NAALADase inhibitors. *J. Med. Chem*. **2001**, *44*, 4170−4175. (c) Thomas, A. G.; Vornov, J. J.; Olkowski, J. L.; Merion, V. T.; Slusher, B. S. *N*-Acetylated α-linked acidic dipeptidase converts *N*-acetyl-aspartylglutamate from a neuroprotectant to a neurotoxin. *J. Pharmacol. Exp. Ther*. **2000**, *295*, 16−22. (d) Majer, P.; Jackson, P. F.; Delahanty, G.; Grella, B. S.; Ko, Y. S.; Li, W.; Liu, Q.; Maclin, K. M.; Polakova, J.; Shaffer, K. A.; Stoermer, D.; Vitharana, D.; Wang, E. Y.; Zakrzewski, A.; Rojas, C.; Slusher, B. S.; Wozniak, K. M.; Burak, E.; Limsakun, D.; Tsukamamoto, T. Synthesis and biological evaluation of thiol-based inhibitors of glutamate carboxypeptidase II: Discovery of orally active CCPII inhibitor. *J. Med. Chem*. **2003**, *46*, 1989−1996.

(9) (a) Yamamoto, T.; Nozaki-Taguchi, N.; Sakashita, Y.; Inagaki, T. Inhibition of spinal-*N*-acetylated-α-linked acidic dipeptidase produces an antinociceptive effect in the rat formalin test. *Neuroscience* **2001**, *102*, 473−479. (b) Yamamoto, T.; Nozaki-Taguchi, N.; Sakashita, Y. Spinal *N*-acetyl-α-linked acidic dipeptidase (NAALADase) inhibition attenuates mechanical allodynia induced by paw carrageenan injection in the rat. *Brain Res*. **2001**, *909*, 138−144. (c) Chen, R.-U.; Wozniak, K. M.; Slusher, B. S.; Pan, H.-L. Effect of 2-(phosphono-methyl)-pentanedioic acid on allodynia and afferent ectopic discharges in a rat model of neuropathic pain. *J. Pharmacol. Exp. Ther*. **2002**, *300*, 662−667. (d) Yamamoto, T.; Yaksh, T. L. Comparison of the antinociceptive effects of pre- and posttreatment with intrathecal morphine and MK801, an NMDA antagonist, on the formalin test in the rat. *Anesthesiology* **1992**, *77*, 757−763.

(10) (a) Anderson, K. J.; Monaghan, D. T.; Cangro, C. B.; Namboodiri, M. A. A.; Neale, J. H.; Cotman, C. W. Localization of *N*-acetylaspartylglutamate-like immunoreactivity in selected areas of rat brain. *Neurosci. Lett*. **1986**, *72*, 14−20. (b) Forloni, G.; Grzanna, R.; Blakely, R. R.; Coyle, J. T. Colocalization of *N*-acetylaspartlglutamate in central cholinergic, noradrenergic and serotonergic neurons. *Synapse* **1987**, *1*, 455−460. (c) Moffett, J. R.; Cassidy, M.; Namboodiri, M. A. A. Selective distribution of *N*-acetylaspartylglutamate immunoreactivity in the extrapyramidal system of the rat. *Brain Res*. **1989**, *494*, 255−266. (d) Moffett, J. R.; Palkovits, M.; Namboodiri, M. A. A.; Neale, J. H. Comparative distribution of *N*-acetylaspartylglutamate and GAD_{67} in the cerebellum and precerebellar nuclei of the rat utilizing enhanced carbodiimide fixation and immunohistochemistry. *J. Comp. Neurology* **1994**, *347*, 598−618. (e) Moffett, J. R.; Namboodiri, M. A. A. Differential distribution of *N*-acetylaspartylglutamate and *N*-acetylaspartate immunoreactivities in rat forebrain. *J. Neurocytol*. **1995**, *24*, 409−433.

(11) (a) Galli, T.; Godeheu, G.; Artaud, F.; Desce, J. M.; Pittaluga, A.; Barbeito, L.; Glowinski, J.; Cheramy, A. Specific role of *N*-acetyl-aspartyl-glutamate in the in vivo regulation of dopamine release from dendrites and nerve terminals of nigrostriatal dopaminergic neurons in the cat. *Neuroscience* **1991**, *42*, 19−28. (b) Zhao, J.; Ramadan, E.; Cappiello, M.; Bzdega, T.; Wroblewska, B.; Neale, J. H. NAAG inhibits KCl-induced [^{3}H]-GABA release via mGluR3, cAMP, PKA and L-type calcium conductance. *Eur. J. Neurosci*. **2001**, *13*, 340−346.

(12) (a) Nan, F.; Bzdega, T.; Pshenichkin, S.; Wroblewski, J. T.; Wroblewska, B.; Neale, J. H.; Kozikowski, A. P. Dual function glutamate-related ligands: discovery of a novel, potent inhibitor of glutamate carboxypeptidase II possessing mGluR3 agonist activity. *J. Med. Chem*. **2000**, *43*, 772−774. (b) Kozikowski, A. P.; Nan, F.; Conti, P.; Zhang, J.; Ramadan, E.; Bzdega, T.; Wroblewska, B.; Neale, J. H.; Pshenichkin, S.; Wroblewski, J. T. Design of remarkably simple, yet potent urea-based inhibitors of glutamate carboxypeptidase II (NAALADase). *J. Med. Chem*. **2001**, *44*, 298−301.

(13) (a) Ezquerra, J.; Pedregal, C.; Rubio, A.; Yruretagoyena, B.; Escribano, A.; Sánchez-Ferrando, F. Stereoselective reactions of lithium enolates derived from *N*-BOC protected pyroglutamic esters. *Tetrahedron Lett*. **1993**, *49*, 8665−8678. (b) Coudert, E.; Archer, F.; Azerad, R. A Convenient and efficient synthesis of (2*S*,4*R*)-and (2*S*,4*S*)-4-methylglutamic Acid. *Synthesis* **1997**, 863−865.

(14) Lombart, S. D.; Blanchard, L.; Stamford, L. B.; Tan, J.; Wallace, E. M.; Satoh, Y.; Fitt, J.; Hoyer, D.; Simonsbergen, D.; Moliterni, J.; Marcopoulos, N.; Savage, P.; Chou, M.; Trapani, A. J.; Jeng, A. Y. Potent and selective non-peptidic inhibitors of endothelin-converting enzyme-1 with sustained duration of action. *J. Med. Chem*. **2000**, *43*, 488−504.

(15) Rong, S.-B.; Zhang, J.; Neale, J. H.; Wroblewski, J. T.; Wang, S.; Kozikowski, A. P. Molecular modeling of the interactions of glutamate carboxypeptidase II with its potent NAAG-based inhibitors. *J. Med. Chem*. **2002**, *45*, 4140−4152.

(16) Cruciani, C.; Crivori, P.; Carrupt, P. A.; Testa, B. Molecular fields in quantitative structure−permeation relationships: the VolSurf approach. *J. Mol. Struct*. **2000**, *503*, 17−30.

(17) Pomper, M. G.; Musachio, J. L.; Zhang, J.; Zhou, Y.; Rauseo, P.; et al. C-11-MCG: Synthesis, uptake selectivity and primate PET of a probe for NAALADase/PSMA. *J. Nucl. Med*. **2002**, *43*.

JM0306226